Wavelength modulation waveforms in laser photoacoustic spectroscopy

Jaakko Saarela,* Juha Toivonen, Albert Manninen, Tapio Sorvajärvi,
and Rolf Hernberg

Optics Laboratory, Department of Physics, Tampere University of Technology,
P.O. Box 692, FI-33101 Tampere, Finland

*Corresponding author: jaakko.saarela@tut.fi

Different wavelength modulation waveforms were studied comprehensively in tunable diode laser photoacoustic spectroscopy. The generation of the photoacoustic signal was studied by way of simulations and experiments. A cantilever-enhanced photoacoustic detector and CO_2 sample gas were used in the experiments. The modulation waveforms compared in this study were sinusoidal, triangular, shaped, and quasi-square waves. All four waveforms allow background-free detection of trace gases. Compared to the conventionally used sinusoidal modulation, the triangular, shaped, and quasi-square waves enhanced the photoacoustic signal by factors of 1.12, 1.42, and 1.57, respectively.   © 2009 Optical Society of America

OCIS codes: 300.6260, 300.6430, 300.6380.

1. Introduction

Photoacoustic spectroscopy (PAS) is a sensitive tool for trace gas analysis. In the photoacoustic (PA) effect sample molecules absorb light that is modulated periodically. Because of inelastic collisions between molecules, a portion of the absorbed energy is released as heat to the environment. As a result, an acoustic wave is generated that is then detected with a microphone.

Ultrasensitive PAS techniques take advantage of cantilever-enhanced [1] and quartz-enhanced [2] detection. Very low detection limits have also been achieved with resonant PA cells and high-power lasers [3,4]. In the infrared region of the spectrum where most molecules have their fundamental vibrational bands, tunable, narrowband semiconductor lasers are preferred. Normalized noise-equivalent absorption (NNEA) is often used to compare different methods [5]. The smallest reported NNEA values are $1.9 \times 10^{-9}\,\mathrm{cm}^{-1}\,\mathrm{WHz}^{-1/2}$ for quartz-enhanced PAS [2],
$1.5 \times 10^{-9}\,\mathrm{cm}^{-1}\,\mathrm{WHz}^{-1/2}$ for resonant PA detection [3], and $1.7 \times 10^{-10}\,\mathrm{cm}^{-1}\,\mathrm{WHz}^{-1/2}$ for cantilever-enhanced PAS [5].

Usually, in tunable diode laser PAS (TDLPAS) the emission wavelength of the laser is scanned sinusoidally and symmetrically across the absorption line with a small modulation amplitude. During one scanning period the absorption line of the sample molecules is crossed twice. Thus, a nearly sinusoidal PA signal is generated at twice the modulation frequency ($2f_{\mathrm{mod}}$). In resonant detection the signal frequency is matched to the resonance of the PA detector. Because the walls and windows are broadband absorbers, the PA signal from sample gas is void of acoustic background. Therefore, the background-free wavelength modulation (WM) is often favored over amplitude modulation (AM), which suffers from an interfering background at the PA signal frequency.

In this work, the sensitivity of TDLPAS was studied with a cantilever-enhanced PA detector by using different modulation waveforms. Quasi-square [6], shaped, triangular, and sinusoidal waveforms were used. Conventionally, the sinusoidal modulation

waveform is used, which is not the optimum choice for generation of a PA signal. The novel shaped modulation waveform is tailored for a specific absorption line to produce a sinusoidal PA signal. Compared to the sinusoidal modulation, the obtained results indicate that the triangular, shaped, and quasi-square modulation waveforms improve the PA signal by factors of 1.12, 1.42, and 1.57, respectively. The quasi-square waveform (QSW) gives the largest signal-to-noise ratio (SNR) due to the largest $2f_{mod}$ frequency component in the PA signal.

2. Experimental Setup

A custom nonresonant photoacoustic detector (Gasera Ltd., Turku, Finland) was used in the laboratory experiments. The pressure transducer is a flexible, rectangular cantilever (length 6 mm, width 1.5 mm, and thickness 10 μm), whose bending motion is measured optically with a Michelson interferometer. The cantilever resembles a damped harmonic oscillator. Its vibrational amplitude is directly proportional to the pressure but is also defined by the modulation frequency and the mechanical properties of the detector, which contribute to the sensitivity of the device [1,7]. The inner diameter and the length of the photoacoustic cell were 3 mm and 42 mm, respectively.

Carbon dioxide (CO_2), with a concentration of 5000 ppm in nitrogen (N_2), was used as the sample gas in normal environment [normal temperature and pressure (NTP)] conditions. The measurement setup is shown in Fig. 1. A temperature controller (LDT 5525, ILX Lightwave, Bozeman, Montana) was used for temperature stabilization and coarse wavelength tuning of a distributed-feedback (DFB) diode laser (FOL 15DCWD-A81-19060, Furukawa Electric, Tokyo, Japan). A diode laser current controller (LDX-3320, ILX Lightwave) was modulated by a programmable function generator (33250A, Agilent Technologies, Santa Clara, California) for fine tuning of the laser wavelength. The DFB diode laser has a current tuning parameter of 7.6×10^{-3} nm/mA. The diameter of the collimated laser beam was approximately 1 mm and the average power was 30 mW.

3. Formation of Photoacoustic Signal

In TDLPAS the $2f_{mod}$ frequency component is extracted from an amplitude spectrum of the PA signal. The amplitude at the signal frequency is a product of
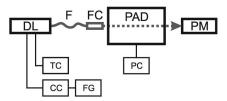

Fig. 1. Measurement setup: DL, fiber-pigtailed DFB diode laser; F, optical fiber; FC, fiber collimator; PAD, photoacoustic detector; PM, powermeter; TC, temperature controller; CC, current controller; FG, function generator; and PC, personal computer. The gas exchange system is not shown.

the detector sensitivity, the absorption coefficient of the gas, and the laser power [8]. The signal depends also on the manner in which the laser wavelength is tuned across the absorption line.

In semiconductor diode lasers the wavelength is usually tuned by adjusting the injection current. A sinusoidal, small-amplitude tuning across the absorption line center produces an acoustic signal, having most of the energy at frequency $2f_{mod}$. However, when the amplitude of the tuning is increased, harmonic frequencies of $2f_{mod}$ are added to the signal and the signal is no longer sinusoidal. This is caused by the nonlinear-shaped absorption profile, which is modeled with a Voigt function in general. Furthermore, if the amplitude of the sinusoidal modulation is increased beyond a certain range, the $2f_{mod}$ signal component saturates and begins to decrease [9–12].

The magnitude of modulation is often described with a unitless modulation index, also referred to as a modulation depth. The modulation index is defined as a peak-to-peak modulation amplitude divided by the absorption linewidth (FWHM) of the molecule [6]. Intuitively, the PA signal would reach its maximum when the modulation index is much larger than 1. With a large modulation index the absorption is varied between zero and the maximum value at the line center. For the sinusoidal modulation the optimum modulation index is about 2.2 [6]. Beyond this value a remarkable portion of the $2f_{mod}$ signal is redistributed to the higher harmonics. Thus, the best choice is to use the optimum modulation index and to measure only the $2f_{mod}$ component, which usually has the best SNR.

One way to improve the $2f_{mod}$ signal component is by using a novel shaped modulation waveform. Under an assumption of a very narrow laser line and weak absorption, the PA signal is directly proportional to the absorption coefficient of the sample gas at the laser frequency, $\alpha(\nu_L - \nu_0)$. The absorption profile can be determined experimentally with a linear wavelength scan. However, in this work, the absorption profile was calculated from the known line-broadening parameters of CO_2. Once the shape of the absorption is known, one can tailor a shaped modulation waveform that yields a pure sinusoidal PA signal in TDLPAS. The shaped modulation waveform and its PA response is shown in Fig. 2. A PA response for a linear, triangular modulation waveform is also shown. For simplicity, the frequency response of the PA detector was omitted in the simulations. The shaped waveform in Fig. 2 was calculated from an assumed Voigt-like absorption of CO_2, which is a convolution of Lorentz and Doppler profiles. At the transition wavelength of 1572 nm, i.e., at 6361 cm^{-1}, and in normal environment, the linewidth (FWHM) of the pressure-broadened Lorentzian is 0.1428 cm^{-1} [13], whereas the Doppler linewidth [14] is only 0.0118 cm^{-1}. Thus, the Voigt profile resembles a Lorentzian closely. The absorption cross section at the line center is 7.5×10^{-23} cm^2/molecule.
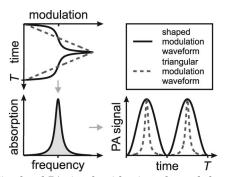
Fig. 2. Simulated PA signals with triangular and shaped modulation waveforms. The modulation index, i.e., the peak-to-peak modulation amplitude with respect to the absorption linewidth (FWHM), is 10. Triangular scan yields a pure absorption spectrum from which the shaped modulation waveform is calculated. The shaped modulation waveform produces a pure sinusoidal PA signal with all the absorbed energy concentrated into a single signal frequency.

4. Results and Discussion

The PA responses of four different modulation waveforms, a quasi-square, shaped, triangular, and sinusoidal, were compared by way of simulations and experiments. The quasi-square wave, which was originally introduced [6] and implemented [15] for wavelength modulation in absorption spectroscopy, is a symmetric, three-level staircase. The laser frequency switches between the values $\nu_0 - \Delta\nu$, ν_0, and $\nu_0 + \Delta\nu$, where $\Delta\nu$ is the modulation amplitude, in such a way that the absorption maximum is crossed twice during a modulation period.

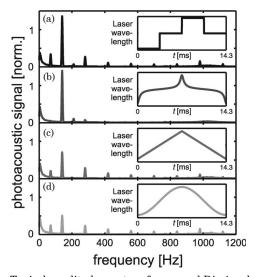Experimental PA spectra, recorded for the different modulation waveforms, are presented in Fig. 3.

Fig. 3. Typical amplitude spectra of measured PA signals with a large laser modulation index, being about 10 in these spectra. The modulation waveforms are (a) quasi-square wave (QSW), (b) shaped wave, (c) triangular wave, and (d) sinusoidal wave, which are shown in the insets. The fundamental PA signal frequency $2f_{\mathrm{mod}} = 140\,\mathrm{Hz}$ The spectra are normalized with an amplitude that is produced by the sinusoidal modulation at an optimum modulation index of 2.2.

The insets show one period of each modulation waveform. The modulation frequency was set to $70\,\mathrm{Hz}$. Thus, the fundamental $2f_{\mathrm{mod}}$ signal frequency was $140\,\mathrm{Hz}$. Several higher harmonics of $2f_{\mathrm{mod}}$ are seen below the resonance frequency of the cantilever ($1\,\mathrm{kHz}$), beyond which the PA response of the detector is substantially reduced. Each PA spectrum in Fig. 3 is an average of 100 fast Fourier transform (FFT) spectra, each of which is calculated from a PA signal of $300\,\mathrm{ms}$ in duration. The laser wavelength was scanned symmetrically across the rotational absorption line with a modulation index of about 10. The modulation index was determined by multiplying the laser tuning parameter with the peak-to-peak current modulation amplitude and dividing that by the known linewidth (FWHM) of the Voigt-shaped absorption profile.

Fourier analysis and background measurements, not shown, prove that all four waveforms are background-free at $2f_{\mathrm{mod}}$. The PA signal itself is generated at even harmonics of f_{mod}, i.e., at $2f_{\mathrm{mod}}$, $4f_{\mathrm{mod}}$ etc. Despite the fact that the current modulation of a diode laser always produces a combined AM–WM, all the waveforms generate a background signal at odd harmonics. The reason for this is that symmetric waveforms consist only of odd harmonics.

The effect of the modulation amplitude was studied experimentally by varying the modulation index between the values of 0.34 and 14.8. A PA spectrum was recorded for each modulation index and waveform. The measured amplitude values at $2f_{\mathrm{mod}}$ as a function of modulation index are presented as dots in Fig. 4. The solid curves are simulated signal amplitudes where an ideal WM is assumed. The calculated curves for the quasi-square, triangular, and sine waves are similar, as presented in Iguchi's work [6]. Both the measured and the simulated curves are normalized with the maximum responses of the sinusoidal excitation at $2f_{\mathrm{mod}}$.
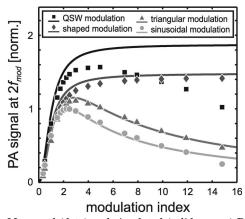

Fig. 4. Measured (dots) and simulated (solid curves) PA signal amplitudes, produced by the four modulation waveforms, at the frequency of $2f_{\mathrm{mod}}$. Pure WM was assumed in the simulations. Wavelength chirp of the diode laser increases with increasing modulation index. Because the QSW modulation suffers the most from the chirp, there is a discrepancy between the modeled and the observed curves at large modulation indices.

The QSW modulation produces approximately an 11% signal improvement compared to the shaped modulation, and nearly 41% and 57% enhancements relative to both triangular and sinusoidal modulations, respectively. With the shaped modulation, the signal level reaches a plateau, whereas sinusoidal, triangular, and quasi-square waveforms give rise to local maxima at modulation indices of 2.2, 3, and 5, respectively. The novel shaped modulation suppressed higher harmonic frequencies very efficiently and it increased the PA signal at $2f_{mod}$ with 42% relative to the sinusoidal modulation. This means a reduction of the detection limit by a factor of 0.7 compared to the limit with optimum sinusoidal modulation. Correspondingly, the QSW modulation reduced the detection limit by a factor of 0.6. The results are summarized in Table 1.

Iguchi has shown theoretically that, in absorption WMS, the second harmonic signal with a sinusoidal modulation, at the line center of a Lorentzian profile, reaches its maximum at a modulation index of about 2.2. In the same article the optimum modulation index for a triangular wave was about 2.8. The QSW modulation gives an absorption enhancement of about 90%, which remains constant at large modulation indices. The QSW modulation produces a square wave absorption and, therefore, has the largest $2f_{mod}$ signal component [6].

The absorption waveforms are the same in both WMS and TDLPAS at the line center. In Fig. 4 the detected amplitude as a function of modulation index with the sinusoidal and triangular waveforms are the same as reported for WMS. However, the experimental curve with the QSW modulation is different at large modulation indices. According to the simulations, the QSW modulation should enhance the signal with about 84%, whereas the enhancement achieved experimentally in this work was only 57%. The discrepancy and the decreasing response of the QSW modulation is due to the fact that the wavelength of the DFB diode laser chirps. During a step modulation the wavelength tuning is not instantaneous but is delayed. Chirping is a well-known effect with DFB diode lasers and, depending on the laser characteristics, the thermal setting times can vary from submicroseconds to several milliseconds, whereas the photon density in the active region is set to within a few nanoseconds [16,17]. Interferometric measurements showed that the wavelength of the DFB diode laser used in this work tuned exponentially to the resonance with a time constant of 0.4 ms, independent of the current modulation step. With 70 Hz QSW modulation, the modulation current is constant for 3.6 ms. Thus, the larger the modulation index, the longer it takes to reach the maximum absorption. Therefore, the absorbed power as a function of time is a distorted square wave whose amplitude at $2f_{mod}$ decreases with increasing modulation index. The wavelength chirp was less significant at $2f_{mod}$ below 20 Hz. However, at such low frequencies the background noise from building vibrations is increased, decreasing the SNR of the PA detection. Optimum modulation frequencies of each modulation waveform were not explored in this study. Neither was the sensitivity of the PA detector optimized.

In contrast to the QSW modulation, all the other modulation waveforms produced PA signals as predicted by the simulations. These waveforms do not show discontinuities that are prone to chirp. However, the wavelength chirp can explain why a small portion of the PA signal, with the novel shaped modulation waveform, was redistributed to $4f_{mod}$ even though chirp occurs mainly far away from the absorption maximum. The reduced effect of the chirp, the insensitivity to the magnitude of the modulation current, and the enhanced sensitivity, compared to the sinusoidal modulation, make the shaped modulation waveform attractive for PA devices.

Despite the fact that a nonresonant PA detector was used in this research, the results are applicable to all kinds of PA device. This is assumed because the PA signal is always directly proportional to the absorbed power. Therefore, in a resonant PA cell, the different waveforms will generate standing pressure waves with similar relative strengths, as shown in Table 1. At very low modulation frequencies or with diode lasers, which exhibit negligible wavelength chirp, the QSW modulation waveform can nearly double the PA signal compared to the sinusoidal modulation. If AM has to be used instead of WM, as with gases absorbing within a broad wavelength band, the obtained results are not directly applicable. In the AM case, a simple square wave, with a duty cycle of 50%, will produce the largest signal because it has the largest $1f_{mod}$ frequency component.

Table 1. Experimental Results with Different Modulation Waveforms Using $f_{mod} = 70$ Hz and $f_{sig} = 2f_{mod} = 140$ Hz

	Waveforms			
	Quasi-Square	Shaped	Triangular	Sinusoidal
PA signal [norm.][a]	1.57[b]	1.42	1.12	1.00
CO_2 detection limit [ppm]	57	63	80	90
NNEA [10^{-8} cm^{-1} WHz$^{-1/2}$]	0.85	0.94	1.20	1.35
Optimum modulation index	5.0	≥8	3.0	2.2

[a]The PA signals are normalized with the maximum signal produced by the sinusoidal modulation at the optimum modulation index of 2.2.

[b]Simulated prediction is 1.84, which was not achieved experimentally because of the wavelength chirp of the DFB diode laser.

5. Conclusions

Photoacoustic spectroscopy is an established method for trace gas analysis. In the infrared part of the spectrum, where molecules have narrow absorption lines, the PA signal is preferably excited with tunable, single-mode semiconductor lasers. The wavelength scanning enables a background-free PA detection at the signal frequency of $2f_{mod}$.

Usually, sinusoidal wavelength modulation is preferred due to its simple use. There are, however, other modulation waveforms that enhance the sensitivity of the PA detector. In this research, four different modulation waveforms were studied by way of simulations and experiments. The waveforms were sinusoidal, triangular, shaped, and quasi-square waves. All the waveforms produce PA signals that are void of acoustic background, which is due to the light absorption at the cell windows and walls.

The shaped modulation waveform developed in this work takes into account the Voigt profile of absorption lines and produces a pure sinusoidal PA signal. Compared to the sinusoidal modulation, the novel waveform increased the signal by a factor of 1.42 when modulation indices larger than 8 were used. Correspondingly, the quasi-square waveform (QSW) produced 1.57 signal enhancement and reduction of the detection limit by a factor of 0.64. Ideally, the QSW modulation should increase the PA signal by a factor of 1.84. This was not achieved because the laser exhibited relatively slow wavelength tuning under the QSW modulation.

The findings of this work apply to all PA systems where wavelength modulation is employed. The QSW modulation gives the largest PA signal with lasers that exhibit negligible wavelength chirp at the modulation frequency used. The novel shaped modulation waveform is also a good choice because of the reduced effect of the chirp, the insensitivity to the magnitude of the modulation current, and the enhanced sensitivity compared to the conventionally used sinusoidal modulation.

References

1. V. Koskinen, J. Fonsen, K. Roth, and J. Kauppinen, "Progress in cantilever enhanced photoacoustic spectroscopy," Vib. Spectrosc. **48**, 16–21 (2008).
2. A. Kosterev, G. Wysocki, Y. Bakhirkin, S. So, R. Lewicki, M. Fraser, F. Tittel, and R. Curl, "Application of quantum cascade lasers to trace gas analysis," Appl. Phys. B **90**, 165–176 (2008).
3. M. E. Webber, M. Pushkarsky, and C. K. N. Patel, "Fiber-amplifier-enhanced photoacoustic spectroscopy with near-infrared tunable diode lasers," Appl. Opt. **42**, 2119–2126 (2003).
4. T. Fink, S. Büscher, R. Gäbler, Q. Yu, A. Dax, and W. Urban, "An improved CO_2 laser intracavity photoacoustic spectrometer for trace gas analysis," Rev. Sci. Instrum. **67**, 4000–4004 (1996).
5. V. Koskinen, J. Fonsen, K. Roth, and J. Kauppinen, "Cantilever enhanced photoacoustic detection of carbon dioxide using a tunable diode laser source," Appl. Phys. B **86**, 451–454 (2007).
6. T. Iguchi, "Modulation waveforms for second-harmonic detection with tunable diode lasers," J. Opt. Soc. Am. B **3**, 419–423 (1986).
7. J. Kauppinen, K. Wilcken, I. Kauppinen, and V. Koskinen, "High sensitivity in gas analysis with photoacoustic detection," Microchem. J. **76**, 151–159 (2004).
8. V. S. Letokhov and V. P. Zharov, *Laser Optoacoustic Spectroscopy* (Springer-Verlag, 1986).
9. H. Cattaneo, T. Laurila, and R. Hernberg, "Photoacoustic detection of oxygen using cantilever enhanced technique," Appl. Phys. B **85**, 337–341 (2006).
10. G. Wysocki, A. Kosterev, and F. Tittel, "Influence of molecular relaxation dynamics on quartz-enhanced photoacoustic detection of CO_2 at $\lambda = 2\,\mu$m," Appl. Phys. B **85**, 301–306 (2006).
11. J.-P. Besson, S. Schilt, E. Rochat, and L. Thévenaz, "Ammonia trace measurements at ppb level based on near-IR photoacoustic spectroscopy," Appl. Phys. B **85**, 323–328 (2006).
12. R. Lewicki, G. Wysocki, A. Kosterev, and F. Tittel, "Carbon dioxide and ammonia detection using $2\,\mu$m diode laser based quartz-enhanced photoacoustic spectroscopy," Appl. Phys. B **87**, 157–162 (2007).
13. L. S. Rothman, D. Jacquemart, A. Barbe, D. C. Benner, M. Birk, L. R. Brown, M. R. Carleer, C. Chackerian, Jr., K. Chance, L. H. Coudert, V. Dana, V. M. Devi, J.-M. Flaud, R. R. Gamache, A. Goldman, J.-M. Hartmann, K. W. Jucks, A. G. Maki, J.-Y. Mandin, S. T. Massie, J. Orphal, A. Perrin, C. P. Rinsland, M. A. H. Smith, J. Tennyson, R. N. Tolchenov, R. A. Toth, J. Vander Auwera, P. Varanasi, and G. Wagner, "The HITRAN 2004 molecular spectroscopic database," J. Quant. Spectrosc. Radiat. Transfer **96**, 139–204 (2005).
14. O. Svelto, "Inhomogeneous broadening," in *Principles of Lasers*, 4th ed. (Springer, 1998), pp. 48–49.
15. A. Fried, J. Drummond, B. Henry, and J. Fox, "Versatile integrated tunable diode laser system for high precision: application for ambient measurements of OCS," Appl. Opt. **30**, 1916–1932 (1991).
16. M. Ito and T. Kimura, "Stationary and transient thermal properties of semiconductor laser diodes," IEEE J. Quantum Electron. **17**, 787–795 (1981).
17. W. Li, X. Li, and W.-P. Huang, "A traveling-wave model of laser diodes with consideration for thermal effects," Opt. Quantum Electron. **36**, 709–724 (2004).